TRAK proteins encode distinct MIRO-dependent and MIRO-independent mechanisms for associating with the mitochondrial outer membrane

Lili Mitchell, Kathryn E. Reda, Hijab Fatima, Claudia E. Vasquez, and Omar A. Quintero-Carmona

Department of Biology, University of Richmond, VA 23173

Corresponding author:

Omar A. Quintero-Carmona
Department of Biology
University of Richmond
138 UR Drive
Richmond, VA 23173
Office: (804)287-6892
Lab: (804) 289-1706
FAX (804) 289-8233
Email: oquinter@richmond.edu

I. Abstract

Mitochondria are essential to proper cell function, mislocalization of mitochondria leads to disease. Previous research has indicated that MYO19, an unconventional myosin, localizes to the mitochondria outer membrane (MOM) and enables actin-based mitochondrial movement along the cytoskeleton. MOM insertion of MYO19 is assisted by the small GTPase MIRO, a "molecular switch" that facilitates MYO19/mitochondria interactions. MIRO serves as a "recruiter" of MYO19 to the MOM, rather than the tether/receptor that mediates attachment, as MYO19 contains a second, MIRO-independent mitochondrial association domain. MIRO proteins have previously been reported to serve as attachment points for the microtubule-based motors through interactions with the adaptor protein, TRAK. Past research has identified a MIRO-binding domain of TRAK ($TRAK^{MBD}$) that directly participates in the interaction with MIRO. We chose to investigate whether the interactions between TRAK and MOM paralleled our hypothesized mechanism for MYO19/MOM interactions by examining the MIRO-mediated enhancement of TRAK protein localization to mitochondria, by identifying the location of a MIRO-independent mitochondrial association domain in the c-terminus of TRAK proteins, and by examining the steady-state binding kinetics of various TRAK constructs to mitochondria. We interpret these data to indicate that MIRO proteins serve in the initial recruitment of TRAK proteins to mitochondria, but that the MIRO-independent domain plays a significant role in long-term association between TRAK and MOM.

II. Introduction

Mitochondrial localization is essential to maintaining cellular health

Mitochondria, the powerhouse of the cell, serve many biological roles. In addition to adenosine triphosphate (ATP) synthesis, mitochondria participate in intracellular calcium homeostasis, regulate reactive oxygen species, and are central to apoptotic activities (Wang & Youle 2009). The proper positioning of mitochondria within cells is essential for these activities and for maintaining cellular health. Improper localization can contribute to abnormal mitochondrial functioning which may lead to degenerative diseases, metabolic diseases, and cancer (Wallace 1999). Mitochondria positioning defects are implicated in neuronal dysfunction linked to Alzheimer's and Parkinson's disease (DiMauro et al. 1999). The study of mitochondrial localization mechanisms is therefore important in understanding normal health and physiology, as well as providing foundational understanding for developing treatment options for many serious diseases.

Intracellular transport of mitochondria

Mitochondria localize to different regions of the cell through interactions with the networks of microtubules and actin filaments that form the internal cytoskeleton. Motor proteins attached to the mitochondria move along the different filament systems, utilizing them as tracks to transport the mitochondria throughout the cell. Previous research suggests that different combinations of filaments and motors support different types of transport. Scientists speculate that mitochondria travel along microtubules for long-range transport and along actin filaments for shorter transport distances (Chada & Hollenbeck 2003; Hirokawa & Takemura 2005; Morris & Hollenbeck 1995; Quintero et al. 2009).

Microtubules are tube-like structures formed by the polymerization of α-tubulin and β-tubulin heterodimers (Lodish et al. 2000). As a result, microtubules have structural polarity along their length giving them a plus end and a minus end. In nerve axons, the plus end of the microtubule oriented away from the cell body (Rao & Baas 2018). Microtubules are associated with two motor proteins, kinesin and dynein, which detect the polarity of microtubules biasing their movements in particular directions along microtubules.

Kinesin motors involved in mitochondrial transport are primarily plus end-directed motor proteins that function as a microtubule-activated adenosine triphosphatase (ATPase), coupling ATP hydrolysis to force-generation and movement (Coulombe & Fuchs 1990; Heald & McKeon 1990). Kinesin-1, the kinesin motor protein associated with mitochondrial transportation (Schwarz 2013), forms a heterotetramer of two kinesin heavy chains (KHCs) and two kinesin light chains (KLCs) (Heald & McKeon 1990; Cai et al. 2007). Kinesin consists of two globular heads, a stalk, and C-terminal domains. The KHCs make up the two globular heads of the kinesin motor domain that bind directly to the microtubule as well as a coil-rich stalk and C-terminal tail domain (Vikstrom et al. 1992; Okabe et al. 1993). The KLCs are situated by the C-terminal tail of kinesin and specify the cellular cargo associated with the kinesin (Vikstrom et al. 1992; Okabe et al. 1993).

Dynein is another microtubule-activated ATPase motor protein that binds microtubules. These proteins consist of two heavy chains, three intermediate chains, and four light intermediate chains. Dynein motors are thought to be primarily minus-end directed, allowing cellular cargo to travel in the opposite direction of kinesin-based transportation (Lane et al. 1992).

In addition to microtubules, actin filaments also serve as tracks for shuttling intracellular cargo. Actin filaments (F-actin) are comprised of monomers of globular actin (G-actin) oriented

as a coiled-coil of two protofilaments. The asymmetry within the G-actin monomer structure and the regular quaternary assembly of F-actin lends itself to an inherent structural polarity similarly to that of microtubules (Narita & Maéda 2007). Movement along actin filaments occurs through interactions with different myosins, a family of ATP-dependent motor proteins. Actin-based mitochondrial movement is facilitated by interactions with a mitochondria-associated unconventional myosin, MYO19 (Quintero et al., 2009). MYO19 contains an actin-activated ATPase domain (Adikes et al. 2013) which enables plus-end directed movement (Lu et al. 2014). MYO19 association with mitochondria is mediated by two distinct regions within the MYO19 C-terminal MYO19 mitochondrial outer membrane association domain (MyMOMA): a monotopic alpha-helical membrane insertion (Hawthorne et al. 2016; Sheyer et al. 2016) and a MIRO interacting domain (Oeding et al. 2018; Bocanegra et al. 2019).

MIRO facilitates mitochondrial transport

The rho-like GTPases, MIRO1 and MIRO2, found on the mitochondrial outer membrane (Glater et al. 2006; MacAskill et al. 2009), are involved in facilitating motor protein attachment to mitochondria. MIRO proteins insert into the MOM through a C-terminal transmembrane α-helical domain (Fransson et al. 2003). The N-terminus of MIRO is exposed to the cytoplasm. This region consists of an N-terminal GTPase domain and a C-terminal GTPase domain that flank two calcium binding EF hand motifs (Fransson et al. 2003; Guo et al. 2005; Klosowiak et al. 2013). Although MIRO proteins are broadly expressed in many cell types and at different embryonic stages (Bocanegra et al. 2019), much of the research to date has been in the context of MIRO and mitochondrial traffic in neurons.

Small GTPases like MIRO serve as molecular switches that can transfer between nucleotide states, either GTP-bound or GDP-bound. GTPase activity is regulated by guanine nucleotide exchange factors (GEFs) and GTPase-activating proteins (GAPs). GTPase switches take on an “active” conformation when bound to GTP, which is mediated by GEFs stimulating the release of guanosine diphosphate (GDP) to enable guanosine triphosphate (GTP) to bind. Small G-proteins are inactivated when GAP proteins bind and catalyze the hydrolysis of bound GTP to GDP (Jaffe & Hall 2005). To date, there is little evidence identifying proteins associated with MIRO specific GEF and GAP activity. One potential GAP for MIRO is VopE, a *Vibrio cholerae* Type 3 Secretion System delivered effector (Suzuki et al. 2014). VopE was proposed as a MIRO specific GAP due to an observed increase in MIRO GTPase activity in the presence VopE (Suzuki et al. 2014). Two potential MIRO-specific GEFs have been identified, GBF1 and Vimar (Walch et al. 2018; Ding et al. 2016).

Like other small GTPases, the conformation of MIRO proteins in the GTP-bound form is thought to facilitate protein-protein interactions that are far less likely to occur when the MIRO protein is GDP-bound. Thus, GTP-bound MIRO is often considered the “on” or active version while GDP-bound MIRO is considered “off” or inactive. Because MIRO can transfer between GTP- and GDP-bound states, it is capable of interacting with different sets of proteins. The MIRO/MYO19 interaction appears to be enhanced when MIRO is GTP-bound (Bocanegra et al. 2019), but conflicting reports exist suggesting that MIRO interactions with the microtubule motor adaptor, TRAK, may be enhanced in the GTP-bound (Fransson et al. 2003) or GDP-bound state (MacAskill et al. 2009).

Trak enables Miro binding to microtubule protein motors

Originally identified in *Drosophila*, TRAK adaptor proteins (also known as Milton) facilitate binding between MIRO proteins and microtubule-based motors. Two mammalian TRAK proteins have been identified, TRAK1 and TRAK2, which share ~58% amino acid homology (Beck et al. 2002; Iyer et al. 2003). TRAK1 is comprised of 939 amino acids (106 kDa) while TRAK2 is 913 amino acids in length (101 kDa). The N-terminal region of TRAK family proteins contain a kinesin-interacting domain as well as coiled-coil regions that may facilitate homodimerization (Glater et al. 2006; Stowers et al. 2002). TRAK proteins also contain and additional domain that has been shown to interact with MIRO (Glater et al. 2006; van Spronsen et al. 2013; MacAskill et al. 2009, Koutsopoulos et al. 2010).

The precise mechanisms of MIRO, TRAK, and kinesin interactions have not been well established. However, previous studies indicate that TRAK interacts directly with the kinesin through a KHC C-terminal cargo binding domain (Smith et al. 2006). The kinesin binding domain for TRAK2 has been identified between amino acids 128-283 (Brickley & Stephenson 2011). Past research also suggests that TRAK adaptor proteins interact with MIRO at a specific MIRO binding domain (MBD) (MacAskill et al. 2009). For TRAK2, this domain is located between amino acids 476-700 (MacAskill et al. 2009). Literature suggests that this interaction is dependent on the nucleotide state of MIRO. However, it is unclear which MIRO nucleotide state has a higher affinity for TRAK proteins (Schwarz 2013). Some findings suggests that GTP-bound MIRO enhances TRAK localization to mitochondria (Fransson et al. 2003) while other data indicate that GDP-bound MIRO may favor TRAK interactions (MacAskill et al. 2009). Additionally, there is evidence that TRAK may interact with mitochondria independently of its association with MIRO. Recent studies have shown that when TRAK is expressed in cells

lacking endogenous MIRO, TRAK proteins still localize to mitochondria (Lopez-Domenech et al. 2018).

TRAK and MIRO interactions had initially been characterized in kinesin-mitochondria association, but research has also revealed that the two proteins may be necessary for dynein-mediated mitochondrial transport as well. In MIRO mutant flies, regions of the central nervous system comprised of ~50% dendrites lacked mitochondria (Stowers et al. 2002). While the full mechanism of dynein/MIRO interactions has not been well characterized, these data suggest that dynein-mediated motility does contribute to mitochondrial localization.

In considering the mechanism of interaction between mitochondria and MYO19, Bocanegra and colleagues proposed a model where MIRO proteins serve in initial recruitment steps of MYO19 to mitochondria, and that MIRO-independent mechanisms facilitate longer-term docking between the MOM and MYO19 (Bocanegra et al. 2019). The discovery of MIRO-independent TRAK binding to the MOM led us to the hypothesis that MIRO proteins may also serve in a “recruitment” role for TRAK/MOM interactions. We chose a quantitative microscopy approach to analyze the role of MIRO proteins in enhancing TRAK localization to mitochondria. We were able to localize the MIRO-independent MOM binding domain to the C-terminus of both TRAK1 and TRAK2, and our data lend further support to a model where MIRO proteins serve in the initial recruitment of proteins to the MOM, while other interaction mechanisms mediate longer-lived interactions with the mitochondria.

III. Methods

Construct generation

Human mchr-MIRO2 was previously reported (Bocanegra et al. 2019). Mouse GFP-TRAK constructs used in these studies were generated using previously reported GFP-TRAK plasmids (Lopez-Domenech et al. 2018) as a template. Truncations were generated using PFU Ultra II PCR enzyme for megaprimer insertion PCR or deletion mutagenesis PCR, depending on the nucleotide changes required (Geiser et al. 2001). A schematic of the constructs used can be found in Figure 1.

Cell culture and transfection

HeLa cells (Scherer et al. 1953) and MIRO1/2 double-knockout mouse embryonic fibroblasts (MEF^{dko}) (Lopez-Domenech et al. 2018) were grown in DMEM high glucose (ThermoFisher) supplemented with 10% fetal bovine serum (Gemini Bio-products) 50 units/mL penicillin, and 50µg/mL streptomycin. Cells were maintained in a humidified incubator at 37˚C and 5%CO_2. Cells were passaged using 0.25% trypsin-EDTA. For imaging experiments, HeLa cells were grown on 22mm #1.5 glass coverslips. For live-cell experiments MEF^{dko} cells were grown on #1.5 coverslip glass-bottom 35mm dishes.

Cells were transfected with Lipofectamine 3000 (ThermoFisher) using a modified manufacturer's protocol. For all experiments, 3µL of enhancer reagent, 1µg of GFP-tagged construct DNA were mixed with 0.5µg of mchr-tagged construct DNA and diluted in Optimem (ThermoFisher) without serum or antibiotics, in a final volume of 125µL per coverslip. In all experiments, 4µL of Lipofectamine was diluted into 125µL of Optimem without serum or antibiotics and then mixed with the DNA dilution. Complexes were allowed to form for 5

minutes at room temperature. The entirety of the DNA/reagent mix was added drop-wise to a well of a 6-well plate or one glass-bottom dish. Cells were used for experimentation 18 to 30 hours after transfection.

Cell fixation and image acquisition

Transfected cells grown on coverslips were stained with 100nM Mitotracker DeepRed FM diluted in growth media for 10 minutes, and then washed in growth media for 10 minutes. Cells were then fixed in PBS with 4% paraformaldehyde 37˚C. After permeabilization in PBS with 0.5% TritonX-100 for 5 minutes, cells were stained in PBS with 3.3 nM ALEXA plus 405-phallodin for 20 minutes to label the actin cytoskeleton. Coverslips were washed in PBS four times for five minutes and mounted on slides using PBS in 80% glycerol and 0.5% N-propyl gallate. Coverslips were sealed onto slides with Sally Hansen Tough as Nails clear nail polish.

Images were acquired using an Olympus IX-83 microscope and a PLAN APON 60x/1.42NA DIC objective. Cells were illuminated using an EXFO mixed gas light source, Sedat Quad filters (Chroma), and Sutter filter wheels & shutters. Images were acquired using a Hamamatsu ORCA-Flash 4.0 V2 sCMOS camera, and Metamorph imaging software to control the system components. In all instances, exposure times maintained constant across experimental data sets.

Mito/Cyto Ratio calculation

The ratio of mitochondria localized fluorescence to cytosol localized fluorescence (mito/cyto ratio, MCR) was calculated by measuring the mean gray value of mitochondria and

cytosol with 3×3 pixel boxes using FIJI software. The ratio was calculated for five separate regions within one cell and then averaged across the cell.

The assumption of the MCR is that GFP-TRAK fluorescence will evenly disperse throughout the entire cell unless TRAK is specifically targeted to a cellular location, such as the mitochondria. “Mitochondrial regions” of cells were identified by using the Mitotracker channel. Mitochondrial boxes were placed where mitochondria were visible. Boxes were placed for “cytosolic regions” adjacent to mitochondrial boxes in areas of low fluorescence where no mitochondria were present. Measurements were not obtained from the Mitotracker channel. Instead, mito and cyto boxes placed in the Mitotracker channel were applied to corresponding images from the “GFP-TRAK” channel. Because TRAK localization was the primary interest for this study, actual fluorescent measurements were made in the GFP channel. The fluorescence of the mitochondria relative to the fluorescence of the cytosol in the GFP-TRAK channel thus indicated the relative concentration of TRAK proteins in mitochondrial regions compared to the cytoplasm. An MCR that has a value greater than 1 indicates that mitochondria-associated GFP-TRAK fluorescence was greater than cytosolic GFP-TRAK fluorescence. An MCR less than 1 indicates greater cytosolic localization of TRAK than mitochondrial localization. An MCR equal to 1 indicates that TRAK was not localizing differently between the mitochondria and the cytoplasm.

Population analysis of phenotypes

Phenotypic variability exists in any population of cells or organisms. Cells were visually scored to identify the prevalence of strongly localized GFP-TRAK across the population of cells by assigning cells to one of three categories: cytosolic, mitochondrial, or intermediate

localization (Bocanegra et al. 2019). Cells characterized as “cytosolic” cells showed no distinct GFP-TRAK fluorescence in mitochondrial regions, while cells characterized as “mitochondrial” displayed strong fluorescence in mitochondrial regions with little fluorescence in cytosolic regions. “Intermediate” cells exhibited strong fluorescence in mitochondrial regions in conjunction with some fluorescence in cytosolic regions. During population scoring, the data collector was blinded to the identity of the samples. The fraction of cells exhibiting each TRAK localization phenotype was calculated by manually scoring 60-100 cells per coverslip. The percentage of cells of each phenotype was calculated by dividing the number of cells of a specific phenotype by the total number of cells counted for the coverslip.

Fluorescence recovery after photobleaching (FRAP) analysis

Cells were grown on coverslip-glass-bottom dishes prior to transfection as previously described. For live-cell imaging, growth media was exchanged for imaging media (Optimem without phenol red containing 50 units/mL penicillin, and 50μg/mL streptomycin), and cells were maintained in a humidified environment at 37°C and 5% CO_2 using a stage-top OKO-labs incubation chamber. Images were collected on an Olympus FV1200 laser scanning confocal microscope outfitted with a PLAN APON 60x/1.4NA objective at a frame-rate of 1 frame every 4 seconds. After the first 15 frames, regions of interest were illuminated for photobleaching at high laser power for 1 second. FIJI was used to identify regions of interest and calculate average fluorescence intensity for each time point. Relative fluorescence at each time point was measured by determining the fluorescence intensity relative to the frame prior to photobleaching (t = 0s). Data were corrected for photofading due to imaging (Applewhite et al. 2007) and averaged together. The mean gray value relative to t = 0 was plotted over time and fit to the

function $y = a*(1 - e^{-bt}) + c*(1 - e^{-dt}) + e$. The half-life ($t_{1/2}$) was calculated using from the exponential rise function by calculating the value of t when y = 0.5. Immobile fraction was calculated by determining the asymptote being approached at time = 600s.

Quantification, analysis, and statistics

Metamorph (Universal Imaging) and FIJI were used for image analysis. Data points are expressed as means ± standard error of the mean. Data were compared by Student's t-test or Dunnett's analysis using Kaleidagraph. Exponential fits for FRAP analysis were performed using Kaleidagraph. Parameters calculated from exponential fits in the data table are expressed as mean ± the SEM calculated across individual samples. Parameters shown on the graphs are calculated as mean ± the SEM -adjusted fit (Singh et al. 2016), by generating curve fits of the mean + SEM and mean − SEM, and reporting the error as the difference between the value calculated from the mean fit and the value calculated from the SEM-adjusted fit. All images were prepared for publication using FIJI, Metamorph, Photoshop, or some combination of these software packages.

IV. Results and Discussion

Ectopic MIRO2 expression enhances TRAK binding to mitochondria

In our initial experiments, HeLa cells were used to quantify the interactions between MIRO and full-length GFP-TRAK and GFP-TRAK^{MBD} through the determination of the MCR. Transfection conditions were chosen so that levels of ectopic expression were limited. Both of the full-length GFP-TRAK1 and GFP-TRAK2 showed enriched mitochondrial localization relative to cytosolic localization (MCR>1). Inducing ectopic expression of mchr-MIRO2, which raised the amount of MIRO2 present on the mitochondria above normal endogenous levels, enhanced the localization of GFP-TRAK proteins to mitochondria, as indicated by increased MCR compared to cells not expressing mchr-MIRO2 (Fig. 2A). Ectopic expression of mchr-MIRO2 also enhanced GFP-TRAK1^{MBD} and GFP-TRAK2^{MBD} localization to mitochondria. However, without ectopic expression of mchr-MIRO2, no enhancement of mitochondrial localization was observed (Fig. 2B). These data support a MIRO-dependent mechanism of TRAK localization to mitochondria.

HeLa cells express endogenous levels of both MIRO1 and MIRO2, so it may be initially surprising that TRAK^{MBD} constructs did not localize strongly to mitochondria when expressed in the absence of exogenous mchr-MIRO2. As the interaction between TRAK^{MBD} and MIRO2 may be a potentially low-affinity interaction, one interpretation of these results could be that the endogenous levels of MIRO expression in HeLa cells are such that GFP-TRAK^{MBD} binding is not detectable by our experimental method. A second interpretation could be that full-length constructs are primarily interacting with mitochondria through a MIRO-independent mechanism which is easier to detect using our experimental approaches. López□Doménech and colleagues recently reported that ectopically expressed of GFP-TRAK constructs still localized to

mitochondria in fibroblasts isolated from mouse embryos where the MIRO1 and MIRO2 locus have been disrupted (MEF^{dko} cells), suggesting that TRAK proteins contain a mechanism for MIRO-independent interactions with the MOM (Lopez-Domenech et al. 2018).

To further investigate whether the presence of MIRO proteins played a role in TRAK localization to the MOM, we repeated our experiments in the MEF^{dko} cells which lack any endogenous MIRO1 or MIRO2 expression (Lopez-Domenech et al. 2018). Results indicate that full-length GFP-TRAK constructs still display an MCR >1, indicating enhanced mitochondrial localization even in the absence of MIRO expression (Fig. 3A). Ectopic expression of mchr-MIRO2 increased the MCR of full-length GFP-TRAK2, but not of GFP-TRAK1 (Fig. 3A). GFP-$TRAK^{MBD}$ localization was also enhanced by ectopic expression of mchr-MIRO2 but displayed no enhancement in localization without MIRO expression (Fig. 3B). These findings confirm a MIRO-independent mechanism of TRAK localization to mitochondria, and that this interaction may be the dominant mechanism of interaction between TRAK1 and the MOM.

To further characterize the phenotype in a population context rather than an individual cell-context, population phenotype analysis was performed to compare MEF^{dko} cell phenotypes when expressing different combinations of GFP-TRAK and mchr-MIRO2 constructs. These experiments revealed that ectopic expression of mchr-MIRO2 reduced the fraction of cells displaying a cytosolic GFP-TRAK localization phenotype in cells coexpressing mchr-MIRO2 with GFP-TRAK1, GFP-TRAK2, or GFP-$Trak2^{MBD}$, but not for GFP-$TRAK1^{MBD}$ (Fig. 3C). The difference in the population analysis between GFP-$TRAK1^{MBD}$ and GFP-$TRAK2^{MBD}$ could indicate a difference in affinity for MIRO2 between the two TRAK isoforms. Taken together, these data support the notion that a TRAK interaction with mitochondria are at least partially MIRO-independent.

MIRO-independent mitochondrial localization is encoded by the C-terminus of TRAK proteins

To investigate which region of TRAK facilitates MIRO-independent binding, we generated new GFP-TRAK truncation constructs encoding for the N-terminal region before the MBD and the C-terminal region after the MBD in both for both TRAK1 and TRAK2. These constructs were expressed in MEF^{dko} cells, and we measured their localization characteristics (Fig. 4). In agreement with previous experiments, full-length GFP-TRAK1 localizes to mitochondria and had a MCR>1 (Fig. 4A). The N-terminal TRAK1 construct, GFP-$TRAK1^{1-486}$, did not show enhanced mitochondrial localization with a MCR ~1. The C-terminal construct, GFP-$TRAK1^{699-939}$, did display enhanced mitochondrial localization with a MCR >1, but less than that of full-length GFP-TRAK1 (Fig. 4A). Similar results were obtained for GFP-TRAK2 where the N-terminal construct (GFP-$TRAK2^{1-475}$) displayed a MCR ~1 but the C-terminal construct (GFP-$TRAK2^{701-913}$) had a MCR greater than 1 (Fig. 4B). Population phenotype analyses were also performed for each GFP-TRAK construct. Cells expressing the GFP-TRAK N-terminal construct displayed primarily cytosolic fluorescence (Fig. 4C). In contrast, cells expressing either full-length GFP-TRAK or the C-terminal construct had a greater fraction of intermediate and mitochondrial phenotypes, further supporting the presence of a MIRO-independent MOM association domain encoded by the C-terminus of TRAK (Fig. 4C). It is possible that the truncated constructs may not exist in a confirmation that completely recapitulates the ability of the full-length TRAK protein to interact with the mitochondrial membrane, and that the missing sequences in the N-terminal region and/or the MBD may still contribute to some aspects of MIRO-independent TRAK localization to the MOM.

The TRAK domains responsible for MIRO-dependent and MIRO-independent MOM binding have different steady-state turnover kinetics

Fluorescence recovery after photobleaching (FRAP) was performed to determine the kinetic properties of full-length GFP-TRAK/MOM interactions, GFP-TRAK^{MBD}/mchr-MIRO2 interactions, and GFP-TRAK^{cterm}/MOM interactions (Table 1). Full-length GFP-TRAK1 and GFP-TRAK 1^{cterm} expressed in MEF^{dko} cells had a slower rate of exchange compared to that of GFP-TRAK1^{MBD} expressed in combination with mchr-MIRO2 (Fig. 5A). Similar results were observed with GFP-TRAK2 constructs as well (Fig. 5B). GFP-TRAK^{MBD} constructs expressed in combination with mchr-MIRO2 had significantly faster $t_{1/2}$ as well as a significantly smaller immobile fraction, compared to their corresponding full-length construct expressed in the absence of any MIRO. GFP-TRAK^{cterm} constructs displayed FRAP kinetics far more similar to the full-length construct, although their $t_{1/2}$ were not quite as large as those of the full-length constructs.

These analyses suggest that GFP-TRAK^{cterm} interactions with the MOM have a stronger association than the GFP-TRAK^{MBD} interaction with mchr-MIRO2. As the kinetics of full-length GFP-TRAK are also significantly slower than those between GFP-TRAK^{MBD} and mchr-MIRO2, these data suggest that the TRAK^{MBD} interaction with MIRO facilitates an initial, loose recruitment of the mitochondria while TRAK^{cterm} is partially responsible for slower turnover and stronger interactions between TRAK and the MOM. As we observed with the MCR analysis, the quantitative difference between the full-length GFP-TRAK construct and the GFP-TRAK^{MBD}/mchr-MIRO2 interaction is not recapitulated to the same magnitude by the GFP-TRAK^{cterm} construct. This likely indicates that while some other regions of the TRAK protein may not be necessary for MIRO-independent interactions with the MOM, they may still play a

role in enhancing those interactions. Specifically, just as multimerization of motor proteins influences the time-fraction that the proteins are associated with their cytoskeletal filament (Howard 2001), dimerization of TRAK through the N-terminal coiled-coil domains could enhance MOM binding.

V. Conclusions and Future Directions

Current models suggest that MIRO "anchors" TRAK proteins to the mitochondrial membrane (Kruppa & Buss 2021). This interpretation is likely a consequence of experimental design as nearly all of the previous experimental examinations of MIRO/TRAK interactions were carried out as end-point assays. Cells were made to express a set of proteins under particular conditions, and then "fixed in time" for analysis. These analyses included assaying for binding via immunoprecipitation, or for localization via qualitative fluorescence microscopy. These experimental approaches do not address a key component required for full understanding of biologically relevant protein-protein interactions--kinetic descriptors are crucial to informing a more complete biological understanding (Pollard & De La Cruz 2013). Additionally, qualitative image analysis approaches make it more difficult to validate and compare results between experimental conditions (Wait et al. 2020). In taking a quantitative and kinetic approach to our experimental design, we were able to identify biologically relevant differences in the biochemical behavior of different regions of the TRAK proteins with respect to mitochondrial binding.

Population analysis and MCR determination in MEF^{dko} cells not expressing endogenous MIRO enabled us to determine that the C-terminus of TRAK interacted with the MOM (Fig. 4). Fixed-cell endpoint assays also indicated that this interaction likely has different properties than that of the $TRAK^{MBD}$/MIRO interaction. Although the $TRAK^{cterm}$ demonstrated an interaction with the mitochondria, the quantitative MCR analysis suggests that it did not replicate the same behavior of the full-length construct (Fig. 4A). Previous studies using only qualitative analysis methods may have missed these findings. Kinetic approaches to understanding this interaction between $TRAK^{cterm}$ and mitochondria complement findings from the fixed-cell experiments (Fig.

5)—although the C-terminal region is sufficient for MIRO-independent mitochondrial binding, other regions of the TRAK protein may enhance this interaction.

The Quintero lab is currently working to further characterize this MIRO-independent mitochondrial binding domain in the C-terminus of TRAK. To date, the specific mechanism of this interaction is unknown. It is possible that $TRAK^{cterm}$ interacts with the lipids or proteins of the MOM. We and others have previously identified an α-helical domain of MYO19 that inserts into the MOM (Hawthorne et al. 2016; Sheyer et al. 2016), and it is possible that TRAK interacts with the MOM in a similar manner. Sequence analysis of $TRAK^{cterm}$ could reveal an α-helical domain that resembles the membrane-inserting α-helical domain of MYO19, and we could generate GFP-tagged constructs to evaluate its interaction with the MOM. Additionally, it is possible that the coiled-coil regions thought to mediate homodimerization of the TRAK proteins might play a role in enhancing the MIRO-independent binding of TRAK to the MOM. The Q-lab is also in the process of generating GFP-$TRAK^{\Delta MBD}$ constructs, which only lack the MBD domain. If FRAP analysis of these constructs in MEF^{dko} cells resulted in $t_{1/2}$ values of the same magnitude as the full-length TRAK constructs, then these data would indicate that dimerization enhances the MOM binding properties of TRAK.

A revised model for the role of MIRO in motor protein/mitochondria interactions

Kinetic analysis of MYO19/MIRO interactions first revealed that MIRO may provide fast-exchanging binding sites on the MOM for proteins that also contained a second, slower exchanging binding site (Bocanegra et al. 2019). In this way, MIRO provides an initial mechanism of recruitment of MYO19 to the MOM and promotes other MYO19/MOM interactions that are MIRO-independent. This idea is supported by the observations by Oeding

and colleagues as well as Lopez-Domenech and colleagues (Oeding et al. 2018; Lopez-Domenech et al. 2018). Both groups observed that in cells lacking MIRO proteins, MYO19 levels decreased significantly. Their data also supported the interpretation that without MIRO proteins to assist in the insertion of MYO19 with the MOM, MYO19 remains cytosolic where it is accessible to ubiquitination and proteasome-mediated degradation. A similar pattern in FRAP kinetics was observed in the present study for the MIRO/TRAK^{cterm} interactions, suggesting that MIRO may function as an initial recruiter of TRAK but where long-term interactions occur through a MIRO-independent binding mechanism. The impact on degradation kinetics may differ, as loss of MIRO proteins did not obviously impact TRAK protein degradation (Lopez-Domenech et al. 2018).

If MIRO proteins primarily regulate the initial attachment to the MOM and are less involved in long-term association, then the characterization of the nucleotide state dependence of MIRO interactions may need to be reexamined from previous fixed-timepoint experiments. The current model of MIRO activity is that MIRO is active and bound to protein motors in one nucleotide state and inactive in the other nucleotide state, promoting the dissociation of protein motors (Fransson et al. 2003; MacAskill et al. 2009). It is possible however that the nucleotide state dependence of MIRO is not exclusive to turning the “molecular switch” “on” and “off” in order to turn protein motor attachment “on” and “off.” A different interpretation may be that in the active nucleotide state, MIRO simply facilitates recruitment. As MIRO interactions with motors are not the exclusive mechanism of mitochondrial interaction, other mechanisms, such as regulated degradation, would be responsible for controlling motor protein levels on the MOM. To further evaluate the role of MIRO recruitment of mitochondrial motors, then use of point mutations that mimic the different nucleotide states could be used to more carefully examine

which nucleotide state enhances TRAK binding, as we previously examined MIRO/MYO19 interactions (Bocanegra et al. 2019). If MIRO interactions mediate initial recruitment, then other mechanisms may exist that modulate motor protein levels on the MOM. Future investigations could involve kinetic assays to determine the role of ubiquitin-mediated proteolysis pathways on MOM-associated motor protein levels, and if the lifetime of TRAK adaptors and motor proteins on the MOM is sensitive to particular cellular conditions, such as glucose starvation, inner mitochondrial membrane potential, or cell-cycle state. As our experiments reveal that the homeostatic mechanisms regulating motor protein adaptor attachment to the mitochondria are independent of whether MIRO is GTP-bound or GDP-bound, developing a more complete understanding of the additional processes regulating motor protein adaptor attachment will be crucial to understanding the dynamics of mitochondria as an essential organelle in cellular physiology.

VI. Figures and Tables

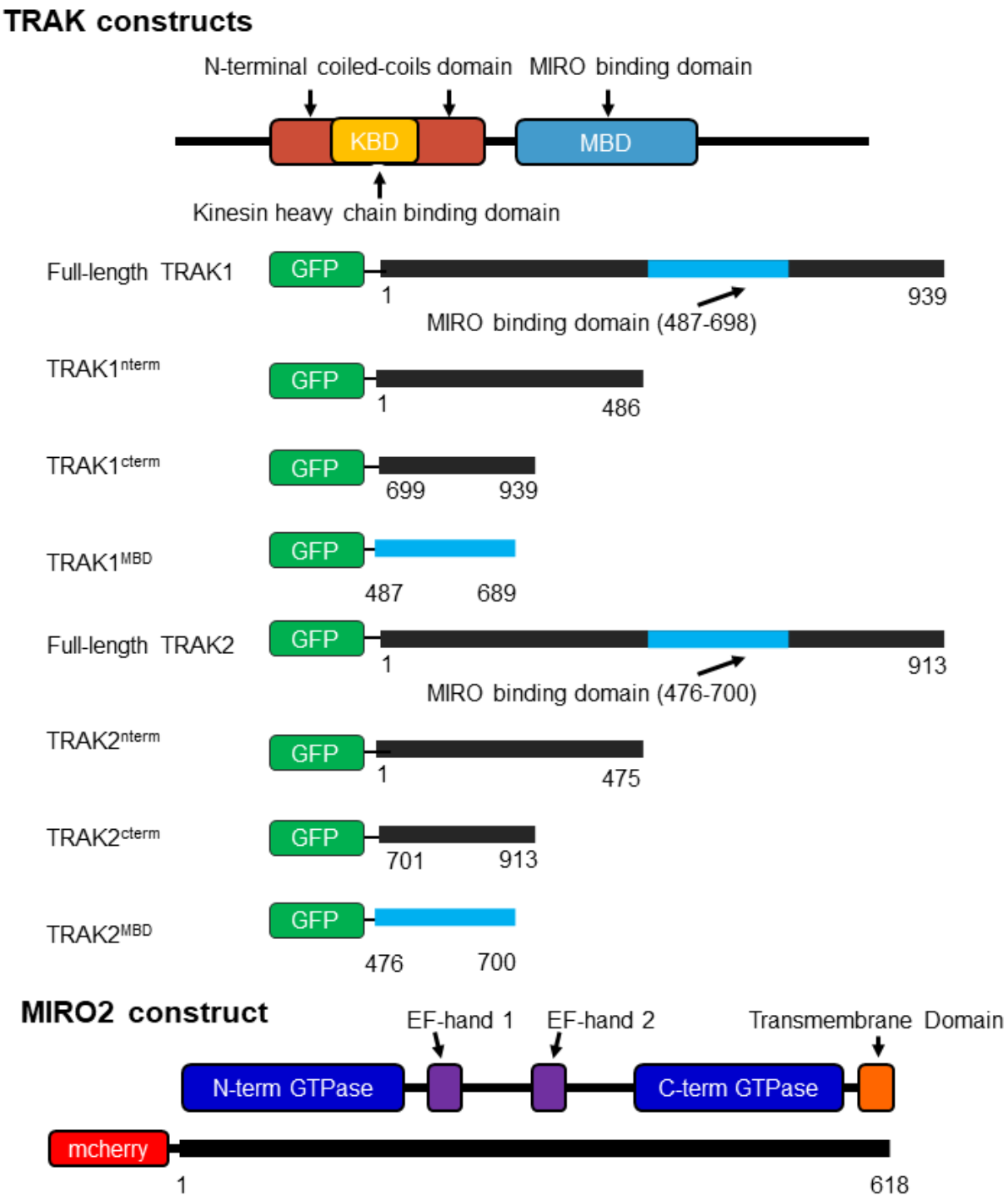

Figure 1: Schematic representations of the TRAK1, TRAK2, and MIRO2 expression constructs used in these studies.

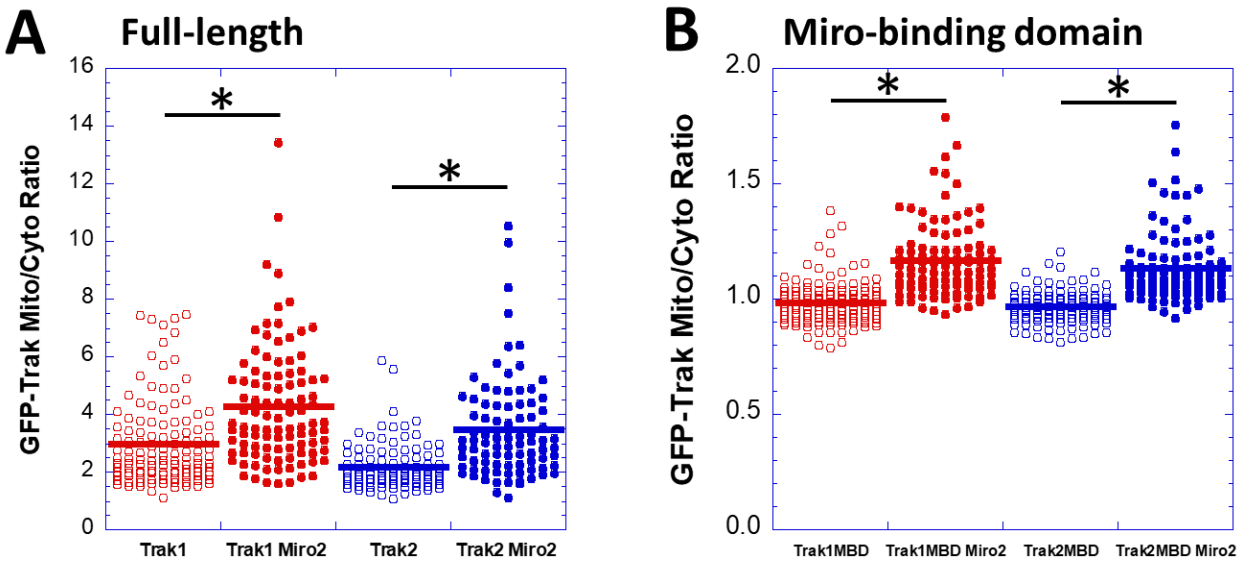

Figure 2: Quantitative image analysis of TRAK1 & TRAK2 localization shows that ectopic expression of mchr-MIRO2 enhances TRAK-binding to mitochondria in HeLa cells. (A) Full length GFP-TRAK1 or GFP-TRAK2 localized more strongly to mitochondria than to the cytoplasm as indicated by a MCR >1. This enrichment was enhanced by ectopic expression mchr-MIRO2 (*$p<0.05$, t-test, $n \geq 86$ cells per condition). (B) GFP-TRAK^{MBD} constructs did not show mitochondrial enrichment (MCR ~1) except when expressed in combination with mchr-MIRO2 expression (*$p<0.05$, t-test, $n \geq 99$ cells per condition).

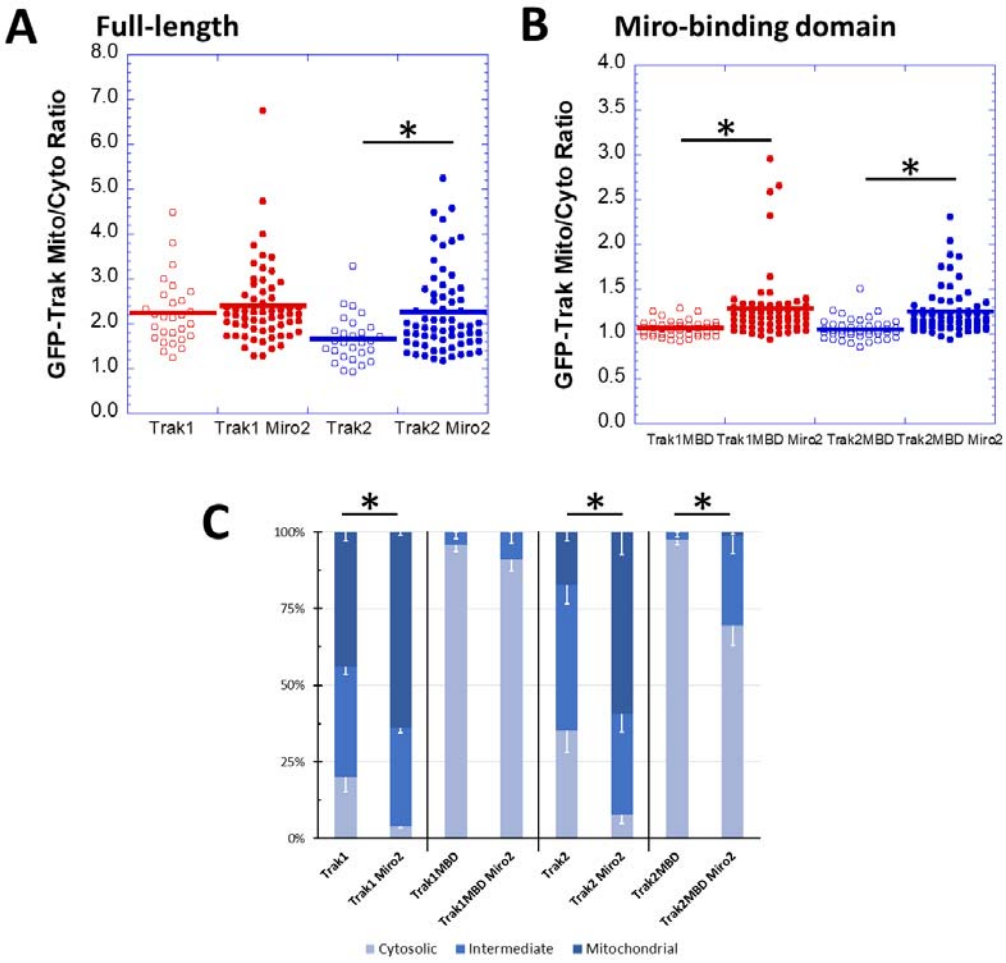

Figure 3: Ectopic mchr-MIRO2 expression modulated GFP-TRAK localization to mitochondria in MEF^{dko} cells. (A) Full length GFP-TRAK1 or GFP-TRAK2 constructs displayed enhanced fluorescence on mitochondria relative to cytoplasm (MCR >1), even in the absence of MIRO expression. Coexpression of mchr-MIRO2 increased the relative brightness of the GFP-TRAK2 fluorescence on mitochondria as compared to the cytoplasm (*$p<0.05$, t-test, n >= 28 cells per condition). (B) GFP-TRAK^{MBD} constructs only displayed enhanced mitochondria fluorescence when coexpressed with mchr-MIRO2 (*$p<0.05$, t-test, n >= 43 cells per condition). (C) Coexpression of mchr-MIRO2 decreased the percentage of cells showing primarily cytosolic localization of GFP-TRAK1, GFP-TRAK2, and GFP-TRAK2^{MBD} (*$p<0.05$, t-test, n >= 4 independent experiments per condition).

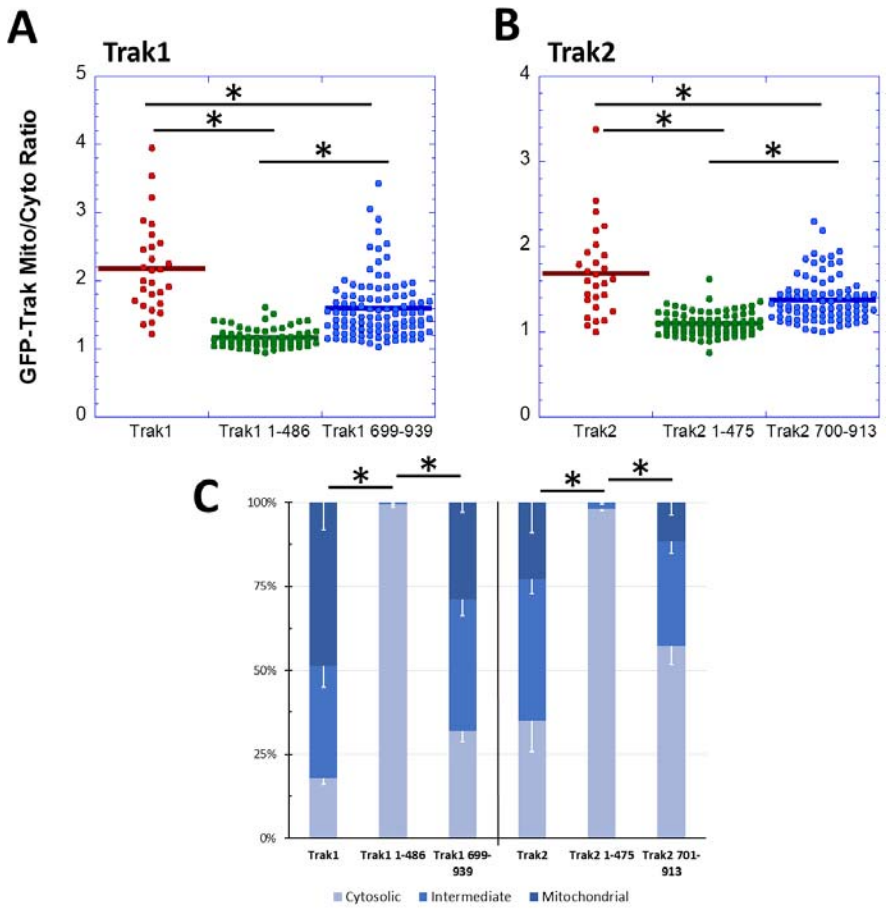

Figure 4: The MIRO-independent mitochondrial localization domain of TRAK is encoded by the amino acids c-terminal of the MIRO-binding domain. (A) GFP-TRAK1$^{699\text{-}939}$ expressed in MEF^{dko} cells displays brighter fluorescence in mitochondrial regions as compared to the cytosol regions (MCR>1), but to a lower degree than GFP-TRAK1. The N-terminal construct, GFP-TRAK1$^{1\text{-}486}$ does not show brighter mitochondrial fluorescence (*$p<0.05$, Dunnett's test compared to full-length, $n \geq 28$ cells). (B) A similar pattern of results was obtained for GFP-TRAK2 constructs and truncations (*$p<0.05$, Dunnett's test compared to full-length, $n \geq 28$ cells). (C) The fraction of cells displaying primarily cytoplasmic fluorescence was smaller for full-length GFP-TRAK or the GFP-TRAK C-terminal constructs as compared to the GFP-TRAK N-terminal constructs (*$p>0.05$, Dunnett's test compared to N-terminal constructs, $n \geq 3$ independent experiments per condition).

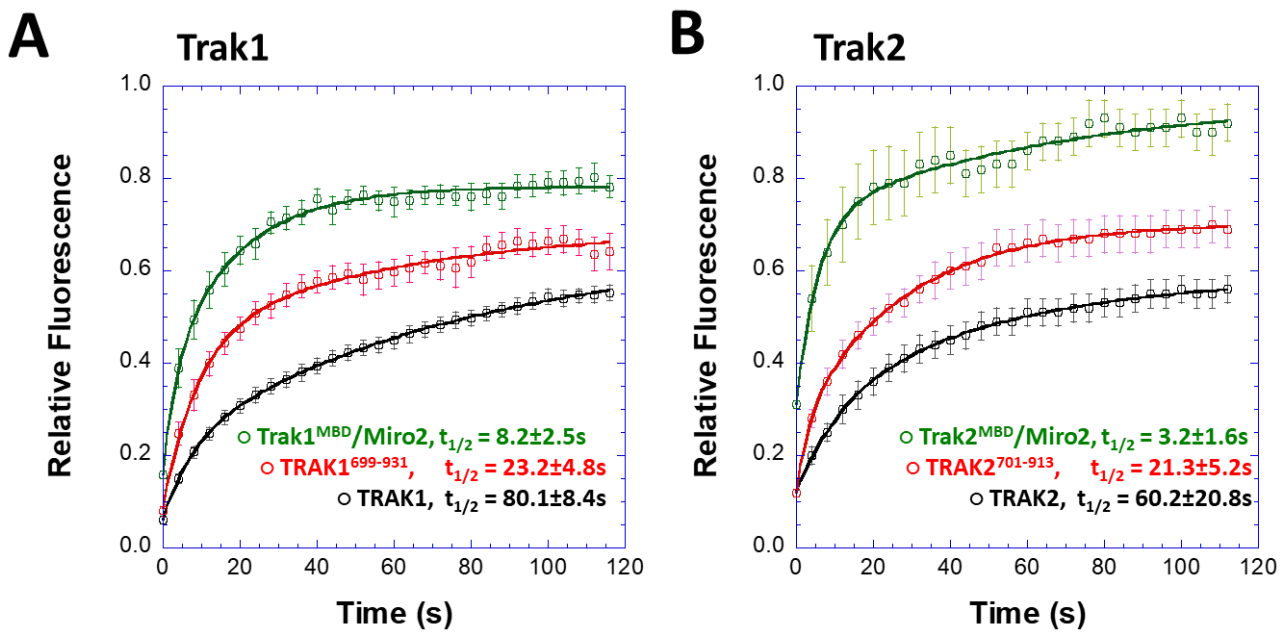

Figure 5: FRAP analysis reveals that GFP-TRAK^{MBD}/mchr-MIRO2 exchange kinetics are faster than MIRO-independent exchange kinetics for other GFP-TRAK constructs. GFP-tagged TRAK 1 (A) and TRAK2 (B) constructs were expressed in MEF^{dko} cells and analyzed for fluorescence recovery after photobleaching. Constructs capable of mitochondrial localization independent of MIRO expression had had significantly larger $t_{1/2}$ and immobile fractions, compared to GFP-TRAK^{MBD} expressed in MEFs coexpressing mchr-MIRO2. See Table 1 for a summary of the analyses for all conditions.

Table 1: FRAP kinetic analysis of GFP-TRAK constructs

	$t_{1/2}$ (s)	Immobile	n
TRAK1	89.8 ± 11.3	0.27±0.03	21
TRAK1$^{699\text{-}931}$	26.2± 3.8*	0.32± 0.04	7
TRAK1^{MBD}/mchr-Miro2	9.4±1.8*	0.17±0.03*	8
TRAK2	98.1 ±26.2	0.25±0.05	14
TRAK2$^{701\text{-}913}$	26.5 ± 8.1*	0.28±0.04	10
TRAK2^{MBD}/mchr-Miro2	18.4 ± 5.7*	0.07 ±0.04*	6

*significantly different from corresponding full-length Trak, $p < 0.05$, Dunnett's test

VII. Acknowledgements

From Lili Mitchell

I would like to thank University of Richmond School of Arts and Science for funding and support. Thank you to all the Q-Lab members whom I have had the opportunity to get to know both inside and outside of the lab. Although our research looked a little different last summer, I wouldn't trade my "summer in FIJI" for a traditional lab experience. A special thanks to Kathryn Reda who stuck with the project & really invested in driving this forward, as well as Claudia Vasquez and Hijab Fatima who rounded out "the TRAK team." Thank you also to Christie Lacy for teaching me to use the Dai Renzu Sama/Olympus microscope. We wouldn't be able to do what we do without you. I would also like to thank Dr. Andrew Moore (HHMI-Janelia), Dr. Rebecca Adikes (Stony Brook University/Siena College), and Dr. Teng-Leong Chew (aka "Scope Shifu," HHMI-Janelia) for giving their time to run out Zoom Image Analysis Bootcamp. It opened the door for nine of us undergrads to be scientists even when we could not be in the lab. And lastly, I would like to thank Dr. Quintero for being the most wonderful mentor I could have ever asked for. Your unconditional support and enthusiasm for science and life (mostly ice cream) is inspirational and I am so thankful to have crossed paths with you at UR.

Hypotheses and experiments in this study were conceived by OAQ and LM. Experiments were performed by LM, and OAQ. Data analysis was completed by LM, KR, HF, CV, and OAQ. Manuscript preparation was completed by LM with assistance from KR and OAQ. This work was funded through University of Richmond Arts & Sciences Summer Fellowships to LM, KR, and CV. HF and OAQ were funded by NIH R15 GM119077 to OAQ. A special thank you to Josef Kittler and Guillermo López-Doménech (University College London) for the MEF^{dko} cells.

VIII. References

Adikes RC, Unrath WC, Yengo CM, & Quintero OA. 2013. Biochemical and bioinformatic analysis of the myosin-XIX motor domain. Cytoskeleton (Hoboken). 70(5): 281–295.

Applewhite DA, Barzik M, Kojima S, Svitkina TM, Gertler FB & Borisy GG. 2007. Ena/VASP proteins have an anti-capping independent function in filopodia formation. Molecular Biology of the Cell, 18(7), 2579–2591

Beck M, Brickley K, Wilkinson HL, Sharma S, Smith M, Chazot PL, Pollard S, Stephenson FA. Identification, molecular cloning, and characterization of a novel GABAA receptor-associated protein, GRIF-1. J Biol Chem. 277(33):30079-90. doi: 10.1074/jbc.M200438200

Bocanegra JL, Fujita BM, Melton NR, Cowan JM, Schinski EL, Tamir TY, Major MB, Quintero OA. 2019. The MyMOMA domain of MYO19 encodes for distinct Miro-dependent and Miro-independent mechanisms of interaction with mitochondrial membranes. Cytoskeleton (Hoboken), 77(3-4), 149-166.

Brickley K & Stephenson FA. 2011. Trafficking kinesin protein (TRAK)-mediated transport of mitochondria in axons of hippocampal neurons. J Biol Chem. 286(20):18079-92. doi: 10.1074/jbc.M111.236018

Cai D, Hoppe AD, Swanson JA, & Verhey KJ. 2007. Kinesin-1 structural organization and conformational changes revealed by FRET stoichiometry in live cells. J Cell Biol. 176(1):51–63. https://doi.org/10.1083/jcb.200605097

Chada SR, Hollenbeck PJ. 2003. Mitochondrial movement and positioning in axons: the role of growth factor signaling. J Exp Biol. 206(Pt 12):1985-92.

Coulombe, PA & Fuchs E. 1990. Elucidating the early stages of keratin filament assembly. J Cell Biol. 111(1):153-169.

DiMauro S. 1999. Mitochondrial encephalomyopathies: Back to mendelian genetics. Ann Neurol. 45: 693-694.

Ding L, Lei Y, Han Y, Li Y, Ji X, & Liu L. 2016. Vimar Is a Novel Regulator of Mitochondrial Fission through Miro. PLoS Genet. 12(10). doi:10.1371/journal.pgen.1006359.

Fransson A, Ruusala A, & Aspenström P. 2003. Atypical Rho GTPases have roles in mitochondrial homeostasis and apoptosis. J Biol Chem. 278(8):6495-502. doi: 10.1074/jbc.M208609200

Geiser M, Cèbe R, Drewello D, & Schmitz R. 2001. Integration of PCR fragments at any specific site within cloning vectors without the use of restriction enzymes and DNA ligase. Biotechniques. 31(1):88-90, 92. doi: 10.2144/01311st05.

Glater EE, Megeath LJ, Stowers RS, & Schwarz TL. 2006. Axonal transport of mitochondria requires milton to recruit kinesin heavy chain and is light chain independent. J Cell Biol. 173(4):545-57. doi: 10.1083/jcb.200601067.

Guo X, Macleod GT, Wellington A, Hu F, Panchumarthi S, Schoenfield M, Marin L, Charlton MP, Atwood HL, & Zinsmaier KE. 2005. The GTPase dMiro is required for axonal transport of mitochondria to Drosophila synapses. Neuron. 47(3):379-93. doi: 10.1016/j.neuron.2005.06.027.

Hawthorne JL, Mehta PR, Singh PP, Wong N, & Quintero OA. 2016. Positively charged residues within the MYO19 MyMOMA domain are essential for proper localization of MYO19 to the mitochondrial outer membrane. Cytoskeleton 73(6):286-299.

Heald R & McKeon F. 1990. Mutations of phosphorylation sites in lamin A that prevent nuclear

lamina disassembly in mitosis. Cell. 61(4):579-89. doi: 10.1016/0092-8674(90)90470-y.

Hirokawa N, Takemura R. 2005. Molecular motors and mechanisms of directional transport in neurons. Nat Rev Neurosci. 6(3):201-14.

Howard J: *Mechanics of Motor Proteins and the Cytoskeleton*. Sunderland, MA: Sinauer Assoc; 2001.

Iyer SPN, Yoshihiro A, & Hart GW. 2003. Identification and Cloning of a Novel Family of Coiled-coil Domain Proteins That Interact with O-GlcNAc Transferase. Journal of Biological Chemistry, 278(7):5399-5409.

Jaffe AB & Hall A. 2005. RHO GTPASES: Biochemistry and Biology. Annual Review of Cell and Developmental Biology, 21(1): 247-269.

Klosowiak JL, Focia PJ, Chakravarthy S, Landahl EC, Freymann DM, & Rice SE. 2013. Structural coupling of the EF hand and C-terminal GTPase domains in the mitochondrial protein Miro. EMBO reports.14(11):968–974.

Koutsopoulos OS, Laine D, Osellame L, Chudakov DM, Parton RG, Frazier AE, Ryan MT. 2010. Human Miltons associate with mitochondria and induce microtubule-dependent remodeling of mitochondrial networks. Biochim Biophys Acta. 1803(5):564-74. doi: 10.1016/j.bbamcr.2010.03.006

Kruppa AJ & Buss F. 2021. Motor proteins at the mitochondria-cytoskeleton interface. *J Cell Sci.134*(7). doi: 10.1242/jcs.226084.

Lane EB, Rugg EL, Navsaria H, Leigh IM, Heagerty AH, Ishida-Yamamoto A, & Eady RA. 1992. A mutation in the conserved helix termination peptide of keratin 5 in hereditary skin blistering. Nature 356, 244–246 (1992). https://doi.org/10.1038/356244a0

Lodish H, Berk A, & Zipursky SL. Molecular Cell Biology. 4th edition. New York: W. H. Freeman; 2000. Section 19.1, Microtubule Structures.

Lopez-Domenech G, Covill-Cooke C, Ivankovic D, Halff EF, Sheehan DF, Norkett R, Birsa N, Kittler JT. 2018. Miro proteins coordinate microtubule- and actin-dependent mitochondrial transport and distribution. EMBO J 37(3):321-336.

Lu Z, Ma XN, Zhang HM, Ji HH, Ding H, Zhang J, Luo D, Sun Y, Li XD. 2014. Mouse myosin-19 is a plus-end-directed, high-duty ratio molecular motor. J Biol Chem. 289(26):18535-48. doi: 10.1074/jbc.M114.569087

MacAskill AF, Brickley K, Stephenson FA, & Kittler JT. 2009. GTPase-dependent recruitment of Grif-1 by Miro1 regulates mitochondrial trafficking in hippocampal neurons. Mol. Cell. Neurosci. 40:301–312

Morris RL, Hollenbeck PJ. 1995. Axonal transport of mitochondria along microtubules and F-actin in living vertebrate neurons. J Cell Biol 131(5):1315-26.

Narita A, Mizuno N, Kikkawa M, & Maéda Y. 2007. Molecular determination by electron microscopy of the dynein-microtubule complex structure. J Mol Biol. 372(5):1320-36. doi: 10.1016/j.jmb.2007.07.046. Epub 2007 Aug 2.

Oeding SJ, Majstrowicz K, Hu XP, Schwarz V, Freitag A, Honnert U, Nikolaus P, & Bähler M. 2018. Identification of Miro1 and Miro2 as mitochondrial receptors for myosin XIX. J Cell Sci. 131(17). doi: 10.1242/jcs.219469.

Okabe S, Miyasaka H, & Hirokawa N. 1993. Dynamics of the neuronal intermediate filaments. J Cell Biol. 121(2):375-86. doi: 10.1083/jcb.121.2.375.

Pollard TD & De La Cruz EM. 2013.Take advantage of time in your experiments: a guide to simple, informative kinetics assays. *Mol Biol Cell 24*(8):1103-10. doi: 10.1091/mbc.E13-

01-0030.

Quintero OA, DiVito MM, Adikes RC, Kortan MB, Case LB, Lier AJ, Panaretos NS, Slater SQ, Rengarajan M, Feliu M and others. 2009. Human Myo19 is a novel myosin that associates with mitochondria. Curr Biol 19(23):2008-13.

Rao AN & Baas PW. 2018. Polarity Sorting of Microtubules in the Axon. Trends Neurosci. 41(2):77-88. doi: 10.1016/j.tins.2017.11.002

Scherer WF, Syverton JT, & Gey GO. 1953. Studies on the propagation in vitro of poliomyelitis viruses. IV. Viral multiplication in a stable strain of human malignant epithelial cells (strain HeLa) derived from an epidermoid carcinoma of the cervix. J Exp Med. 97(5):695-710. doi: 10.1084/jem.97.5.695

Shneyer BI, Ušaj M, & Henn A. 2016. Myo19 is an outer mitochondrial membrane motor and effector of starvation-induced filopodia. J Cell Sci. 129(3):543-56. doi: 10.1242/jcs.175349.

Singh PP, Hawthorne JL & Quintero OA. 2016. Permeabilization activated reduction in fluorescence (PARF): A novel method to measure kinetics of protein interactions with intracellular structures. Cytoskeleton, 73(6), 271–285.

Smith MJ, Pozo K, Brickley K, & Stephenson FA. 2006. Mapping the GRIF-1 binding domain of the kinesin, KIF5C, substantiates a role for GRIF-1 as an adaptor protein in the anterograde trafficking of cargoes. J Biol Chem. 281(37):27216-28. doi: 10.1074/jbc.M600522200

Stowers, RS, Megeath, LJ, Go´rska-Andrzejak J, Meinertzhagen IA, & Schwarz TL. 2002. Axonal transport of mitochondria to synapses depends on milton, a novel Drosophila protein. Neuron. 36:1063–1077.

Suzuki M, Danilchanka O, & Mekalanos JJ. 2014. Vibrio cholerae T3SS effector VopE modulates mitochondrial dynamics and innate immune signaling by targeting Miro GTPases. Cell Host Microbe. 16(5):581-91. doi: 10.1016/j.chom.2014.09.015.

Schwarz TL. Mitochondrial trafficking in neurons. Cold Spring Harb Perspect Biol. 2013 Jun 1;5(6):a011304. doi: 10.1101/cshperspect.a011304.

van Spronsen M, Mikhaylova M, Lipka J, Schlager MA, van den Heuvel DJ, Kuijpers M, Wulf PS, Keijzer N, Demmers J, Kapitein LC, Jaarsma D, Gerritsen HC, Akhmanova A, & Hoogenraad CC. 2013. TRAK/Milton motor-adaptor proteins steer mitochondrial trafficking to axons and dendrites. Neuron. 77(3):485-502. doi: 10.1016/j.neuron

Vikstrom KL, Lim SS, Goldman RD, & Borisy GG. 1992. Steady state dynamics of intermediate filament networks. J Cell Biol. 118(1):121-9. doi: 10.1083/jcb.118.1.121.

Wait EC, Reiche MA, & Chew TL. 2020. Hypothesis-driven quantitative fluorescence microscopy - the importance of reverse-thinking in experimental design. J Cell Sci 133(21):jcs250027. doi: 10.1242/jcs.250027.

Walch L, Pellier E, Leng W, Lakisic G, Gautreau A, Contremoulins V, Verbavatz JM, & Jackson CL. 2018. GBF1 and Arf1 interact with Miro and regulate mitochondrial positioning within cells. Sci Rep. 8(1):17121. doi:10.1038/s41598-018-35190-0

Wallace DC. 1999. Mitochondrial diseases in man and mouse. Science 283(5407):1482-8.

Wang C. & Youle RJ. (2009). The role of mitochondria in apoptosis. Annu. Rev. Genet., 43, 95-118.